GCU Glasgow Caledonian University

University for the Common Good

Sliding mode controller for positioning of an underwater vehicle subject to disturbances and time delays

Tugal, Harun; Cetin, Kamil; Han, Xiaoran; Kucukdemiral, Ibrahim; Roe, Joshua; Petillot, Yvan; Erden, M. Suphi

Published in:
IEEE International Conference on Robotics and Automation

Publication date:
2022

Document Version
Author accepted manuscript

Link to publication in ResearchOnline

Citation for published version (Harvard):
Tugal, H, Cetin, K, Han, X, Kucukdemiral, I, Roe, J, Petillot, Y & Erden, MS 2022, Sliding mode controller for positioning of an underwater vehicle subject to disturbances and time delays. in *IEEE International Conference on Robotics and Automation: ICRA'22.* IEEE, Philadelphia, USA, IEEE International Conference on Robotics and Automation, Philadelphia, Pennsylvania, United States, 23/05/22.

General rights
Copyright and moral rights for the publications made accessible in the public portal are retained by the authors and/or other copyright owners and it is a condition of accessing publications that users recognise and abide by the legal requirements associated with these rights.

Take down policy
If you believe that this document breaches copyright please view our takedown policy at https://edshare.gcu.ac.uk/id/eprint/5179 for details of how to contact us.

Download date: 24. Apr. 2022

CONFIDENTIAL. Limited circulation. For review only.

Sliding Mode Controller for Positioning of an Underwater Vehicle Subject to Disturbances and Time Delays*

Harun Tugal, Kamil Cetin, Xiaoran Han, Ibrahim Kucukdemiral, Joshua Roe, Yvan Petillot, M. Suphi Erden

***Abstract*— Unmanned underwater vehicles are crucial for deep-sea exploration and inspection without imposing any danger to human life due to the extreme environmental conditions. But, designing a robust controller that can cope with model uncertainties, external disturbances, and the time delays for such vehicles is a challenge. This paper implements a sliding mode position control algorithm with a time-delay estimation term to a remotely operated underwater vehicle to deal with disturbances, such as waves, and time delays. The controller is implemented on an underwater vehicle (BlueRov) and compared with a proportional-integral-derivative (PID) controller in a wave tank with different disturbances and when there exist delays within the communication channel. The experimental results show that, the proposed control method provides significantly better performance than the conventional PID in the presence of extreme disturbances.**

I. Introduction

Unmanned underwater vehicles (UUVs) are used for deep-sea exploration, oceanographic data collection, inspecting subsea structures (e.g., pipes, valves, cables within the energy and telecommunication industries), and for military purposes such as to discover and terminate underwater mines. Depending on the complexity and structure of the task, they can either be teleoperated from a ship where the remotely operated vehicle (ROV) continuously communicates with the surface vehicle via a tether/cable or have full autonomy where the autonomous underwater vehicle (AUV) operates without human intervention. The UUVs require a robust controller to accomplish operator commands or to autonomously follow trajectory waypoints under environmental disturbances such as water currents and waves or when there exist time delays within the communication channel [1], [2].

Designing a robust controller for a UUV navigation is a challenging task; model dynamics of the UUV contains high order nonlinearities due to coupling effects and there exist uncertainties due to the limited knowledge of the hydrodynamics and buoyancy forces affecting the system [3]. A designed motion controller needs to be robust, also, to the delays within the system caused by the communication channel or slow data acquisition rate due to the underwater measurement methods such as with sonars [4].

Time delay in control command or sensor measurements is common in underwater applications. With ROV, for instance, the operator usually relies on the visual feedback from the vehicle, which introduces delays due to video transmission and the command signal is also delayed due to the interface and signal transmission from the operator room to the underwater vehicle. With AUVs, the vehicle relies on the Doppler velocity log (DVL) for navigation in shallow waters providing a low rate velocity information. As the DVL relies on the reflected signal from the seabed the data acquisition might vary depending on the distance from the vehicle to the seabed. In general, UUVs can be expected to have a few hundred ms time delays in control commands depending on the application, age of technology used, and the type of the vehicle.

Different types of controllers have been proposed to overcome the aforementioned challenges, for instance in [5] a proportional, integral, and derivative (PID) controller is proposed, which is computationally efficient yet might deliver poor performance under disturbances, for a torpedo shape AUV. In [6] a decoupled PD controller has been proposed as a motion control algorithm. To cope with the translational and turbulence force impacts on a rigid body moving in a fluid, adaptive control methods have been developed as well, see for instance [7], [8], [9], [10], [11], to improve the tracking performance of the UUVs. An Extended Kalman Filter (EKF) adaptive controller utilizing feedback linearization control method has been implemented to a UUV with a manipulator in [10]. Optimal control strategies are also implemented for the motion control of a UUV, see for instance [12] where trajectory following problem of an AUV is formulated as a fixed end point optimal control problem on the euclidean group of motions. In [13], a robust $\mathcal{H}_2$ optimal control method has been developed, taking into account both the environmental disturbances and the time delay for depth control of an AUV.

Sliding mode control (SMC) consists of an algorithm inherently robust to model uncertainties, non-linearities, and external disturbances. It is mostly implemented in vehicle control when the robustness is strictly essential and there exist strong uncertainties in the application [14]. A sliding mode heading controller, compared with a PD controller on the same vehicle, has been proposed for an AUV in [15] with a simplified switching function to reduce actuator wear. In [3], an integral SMC with a time delay estimator has been proposed for an AUVs to cope with the slow data acquisition

*This research was fully funded by EPSRC through the ORCA Hub project with the Grant Reference EP/R026173/1.

H. Tugal and K. Cetin were, X. Han, J. Roe, Y. Petillot, and M. S. Erden are with Institute of Sensors, Signals and Systems, School of Engineering and Physical Sciences, Heriot-Watt University, EH14 4AL, and with Edinburgh Centre for Robotics, Edinburgh, UK. I. Kucukdemiral is with School of Computing, Engineering and Built Environment, Glasgow Caledonian University, G4 0BA, Glasgow, UK. E-mail: harun.tugal@ukaea.uk; kamil.cetin@ikc.edu.tr; x.han@hw.ac.uk; ibrahim.kucukdemiral@gcu.ac.uk; joshua.roe@hw.ac.uk; y.r.petillot@hw.ac.uk; m.s.erden@hw.ac.uk.

Manuscript 402 submitted to 2022 IEEE International Conference on Robotics and Automation (ICRA). Received September 13, 2021.

process and the external disturbances. Dynamic SMC based on the multiple model switching laws has been proposed and implemented in [16] for the depth control of an AUV. In [17], a SMC based on a back-stepping algorithm is proposed to enhance the fault tolerance and the robustness to the external disturbances.

In this paper, a robust SMC with time delay estimator is implemented to control a UUV's position and heading. The performance of the controller is compared with a conventional PID controller as usually used with such underwater vehicles. We have performed experiments in a wave tank to verify the performance of the proposed controller with varying external disturbances and when there exist time delays within the communication channel. The results demonstrate that while both controllers perform satisfactorily in low disturbances, the proposed SMC controller with time delay estimation performs significantly better than the PID in the presence of extreme disturbances.

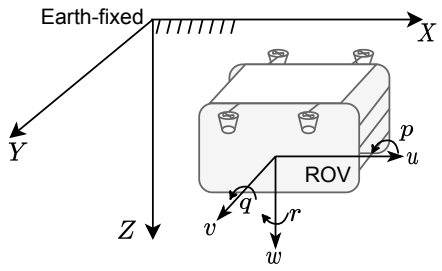

Fig. 1. The vehicle body frame (u, v, w) and the local North, East, and Down (NED) inertial frame (X, Y, Z).

II. Method

The motion of an underwater vehicle in 6 degrees of freedom (DOF) is defined as

$$M\dot{\boldsymbol{\nu}} + C(\boldsymbol{\nu})\boldsymbol{\nu} + D(\boldsymbol{\nu})\boldsymbol{\nu} + \boldsymbol{g}(\boldsymbol{\eta}) = \underbrace{\boldsymbol{\tau}^e + \boldsymbol{\tau}^c}_{\boldsymbol{\tau}}, \qquad (1)$$

where $\boldsymbol{\nu} = \begin{bmatrix} u, v, w, p, q, r \end{bmatrix}^\top$ is the body fixed linear (surge, sway, and heave) and angular (roll, pitch, and yaw) velocity vector, $\boldsymbol{\eta} = \begin{bmatrix} x, y, z, \phi, \theta, \psi \end{bmatrix}^\top$ is the earth fixed position and attitude vector, $\boldsymbol{\tau}^e$ and $\boldsymbol{\tau}^c$ are environmental and control forces and moments acting on the vehicle in the body-fixed frame [18]. Fig. 1 shows the reference frames used in our study. Inertia (encapsulating the added mass), coriolis and centripetal, and hydrodynamic damping matrices are denoted by $M \in \mathbb{R}^{6\times6}$, $C \in \mathbb{R}^{6\times6}$, and $D \in \mathbb{R}^{6\times6}$, respectively. Buoyant and gravitational forces are denoted by the $\boldsymbol{g} \in \mathbb{R}^{6\times1}$ vector. The kinematics equation needs to be included as the control is aimed to provide desired position and attitude in the global reference frame; thus, the relation between the North, East, and Down (NED) frame velocities and body fixed frame can be defined as

$$\dot{\boldsymbol{\eta}} = J(\boldsymbol{\eta})\boldsymbol{\nu}\,,$$

where $J \in \mathbb{R}^{6\times6}$ is the transformation matrix; please refer to [18] for more detailed information. Body frame dynamics of the motion in (1) can be defined in the Earth-fixed inertial frame as

$$M_{\boldsymbol{\eta}}\ddot{\boldsymbol{\eta}} + C_{\boldsymbol{\eta}}(\boldsymbol{\nu},\boldsymbol{\eta})\dot{\boldsymbol{\eta}} + D_{\boldsymbol{\eta}}(\boldsymbol{\nu},\boldsymbol{\eta})\dot{\boldsymbol{\eta}} + \boldsymbol{g}_{\boldsymbol{\eta}}(\boldsymbol{\eta}) = \boldsymbol{\tau}_{\boldsymbol{\eta}}\,,$$

where

$$M_{\boldsymbol{\eta}} = J^{-\top}MJ^{-1}, \quad C_{\boldsymbol{\eta}}(\boldsymbol{\nu},\boldsymbol{\eta}) = J^{-\top}(C - MJ^{-1}\dot{J})J^{-1},$$
$$D_{\boldsymbol{\eta}}(\boldsymbol{\nu},\boldsymbol{\eta}) = J^{-\top}DJ^{-1}, \quad \boldsymbol{g}_{\boldsymbol{\eta}}(\boldsymbol{\eta}) = J^{-\top}\boldsymbol{g}(\boldsymbol{\eta}),$$
$$\boldsymbol{\tau}_{\boldsymbol{\eta}} = J^{-\top}\boldsymbol{\tau}.$$

In this study, the following SMC with a time-delay estimator term, proposed in [19], is applied to an underwater ROV to cope with the external disturbances, uncertainties, and delays

$$\boldsymbol{\tau}^c_{\boldsymbol{\eta}} = \bar{M}\left(\ddot{\boldsymbol{\eta}}_r + K_d^{-1}(K_p\dot{\boldsymbol{e}} + K_i\boldsymbol{e} + \frac{\boldsymbol{s}}{\mu} + \Upsilon\tanh(\frac{\boldsymbol{s}}{\beta}))\right) + k_s(\boldsymbol{\tau}^c_{\boldsymbol{\eta}}(t-L) - \bar{M}\ddot{\boldsymbol{\eta}}(t-L))\,, \qquad (2)$$

where $\bar{M}$ denotes the user defined matrix as $\bar{M} = \text{diag}\left(\bar{m}_x, \bar{m}_y, \bar{m}_z, \bar{m}_\phi, \bar{m}_\theta, \bar{m}_\psi\right)$ with positive parameters ($\bar{m}_i > 0$), μ and k_s are the positive control parameters, $\boldsymbol{\eta}_r$, $\ddot{\boldsymbol{\eta}}(t-L)$, and $\boldsymbol{\tau}^c_{\boldsymbol{\eta}}(t-L)$ denote the reference position trajectory, past vehicle acceleration, and past control effort vectors, respectively. The time-delay estimation is denoted by L, position error is denoted by, $\boldsymbol{e} = \boldsymbol{\eta}_r - \boldsymbol{\eta}$, and $K_j = \text{diag}\left(k_j^x, k_j^y, k_j^z, k_j^\phi, k_j^\theta, k_j^\psi\right)$ denotes the controller gains for $j = p, i, d$. Generally, a signum function is used within a switching control method, yet it is notorious for creating chattering [20]. To eliminate any possible damage on the thrusters due to such chattering, the hyperbolic tangent function, $\tanh(\frac{\boldsymbol{s}}{\beta}) = \left[\tanh(\frac{s_x}{\beta}), \tanh(\frac{s_y}{\beta}), \ldots, \tanh(\frac{s_\psi}{\beta})\right]^\top$, is implemented to calculate the switching with a positive parameter, β, to adjust the sharpness of the boundary layer as in [3].

The sliding surface is calculated as

$$\boldsymbol{s} = K_p\boldsymbol{e} + K_i\int_0^t \boldsymbol{e}(\omega)d\omega + K_d\dot{\boldsymbol{e}}\,,$$

and Υ is calculated as

$$\Upsilon(t) = \delta(\Upsilon(t-L) + K_d\delta_d\mathbf{I} + K_d\delta_c\mathbf{I})(\bar{M} - \delta\mathbf{I})^{-1},$$

where δ, δ_d, and δ_c are positive gains, $\Upsilon(t-L)$ and $\mathbf{I}$ denote the computed past Υ and the identity matrix, respectively. The depicted controller contains a time-delay estimation term that tries to eliminate the effect of the hydrodynamics and disturbances. The vehicle dynamics are relatively cancelled with feedback of delayed control efforts and the acceleration, see [4] for more information about dynamic elimination via inertia matrix and the error convergence. The linear feedback term, with the help of the switching control part, allows the AUV to follow the desired trajectory. Here, in addition to the controller proposed in [3], the position controller contains $\frac{\boldsymbol{s}}{\mu}$ term and K_d^{-1} scaling factor to improve the overall tracking performance. Also, rather than constant, a time variable switching gain matrix, $\Upsilon(t)$, was implemented. A Lyapunov based stability analysis of such SMC is proposed in [3].

Manuscript 402 submitted to 2022 IEEE International Conference on Robotics and Automation (ICRA). Received September 13, 2021.

To compare the proposed controller, a PID controller is also implemented as

$$\boldsymbol{\tau}_{\eta}^{c} = \boldsymbol{s}\,, \tag{3}$$

with slightly different controller gains tuned for a good performance.

Controllers are evaluated based on the Euclidean norm of the recorded position errors with respect to the reference trajectory during the experiment computed as

$$\|E_{xyz\psi}\| = \sqrt{\sum_{i=x}^{l}\sum_{j=1}^{n} e_{ij}^{2}}\,,$$

where the controlled axes are denoted by $l = x, y, z, \psi$ and n denotes the data size. For a t_{max} seconds experiment, with data registration at a rate f_s, the amount of samples recorded will be $n = t_{max} f_s$.

A. Experimental Setup

The proposed control architectures in (2) and (3) were implemented on a BlueROV2 Heavy remotely operated underwater vehicle equipped with a Water Linked DVL A50 (mounted on a tool-skid below the ROV) in a wave tank/pool that can create various types of waves in different magnitudes. Fig. 2 shows the wave tank and the BlueROV in it when centralized type waves were generated during an experiment. The ROV has eight electronic speed controllers (ESCs) and eight Blue Robotics T200 thrusters, four vertically and four horizontally configured at a $\pi/4$ thrust angle, allowing controlling the vehicle in 6 DOF. Fig. 3 shows the location and orientation of the thrusters and Fig. 4 shows the connection of the hardware components. Commands were sent to the ESCs in 30 Hz (f_s) control cycle. The ROV was controlled via the ROS middleware with a computer with a 3.20 GHz CPU connected to the vehicle by a communication tether.

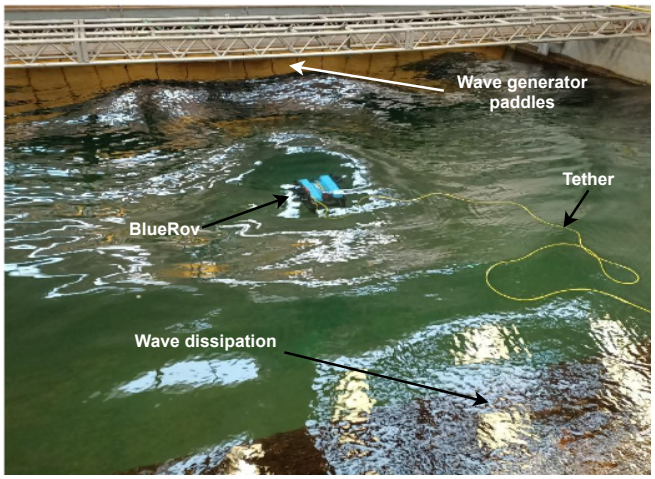

Fig. 2. Wave tank used for the experiments to create environmental disturbances and the BlueROV utilized within the tests.

The distance to the tank floor is measured with a range finder within the DVL and the water depth is measured with a depth sensor mounted on the vehicle. An EKF is used to estimate the relative velocity, position, and orientation of the vehicle based on the other sensors as well, such as Inertial Measurement Unit (IMU), gyroscope, and compass.

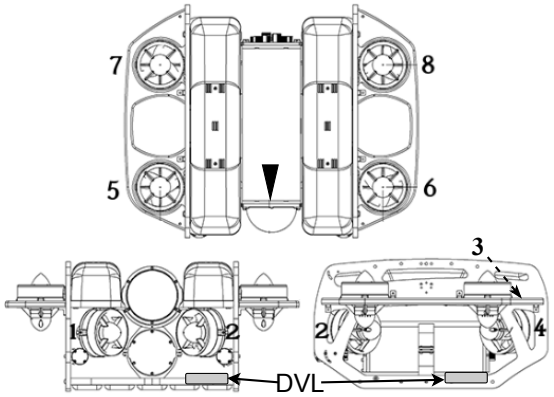

Fig. 3. Bluerov2 Heavy thruster configuration, where thrusters 3, 4, 6, and 7 rotate in clockwise while rest in counter-clockwise, and mounted DVL.

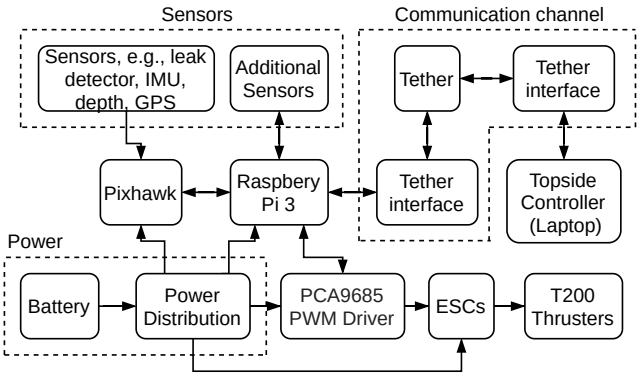

Fig. 4. Block diagram of the hardware components on the BlueROV2 Heavy.

Due to the coupling between different DOF in the system, one could design a controller in 6 DOF for an UUV [9], yet from practical point of view, here, the vehicle position is controlled in 4 DOF, surge, sway, heave, and yaw. This is because almost all underwater vehicles are designed to be inherently stable in pitch and roll; thereby they are operated in 4 DOF. The control input to the thrusters is computed as

$$\boldsymbol{u} = K^{-1} T^{\dagger} \boldsymbol{\tau}^{c},$$

where $T^{\dagger}$ is the generalized inverse of the thruster allocation matrix $T \in \mathbb{R}^{6\times 8}$ which is determined by the layout of all propellers, $K^{-1} \in \mathbb{R}^{8\times 8}$ is the inverse of thrust coefficient matrix, and $\boldsymbol{\tau}^{c}$ is the control effort vector in body fixed frame. The maximum reverse thrust (f_{max}) of the propeller is approximately 40 N; thus, to use normalized controller inputs as $u_i \in [-1, 1]$, the thrust coefficient matrix is assigned as $K = f_{max}\mathbf{I}$.

The thrusters are controlled by pulse width modulation (PWM) signals (signal ranges from 1100 to 1900) sent from a PWM Driver to the ESCs. To achieve direct/single thruster control that the PWM signal for the ESCs is produced by the

Manuscript 402 submitted to 2022 IEEE International Conference on Robotics and Automation (ICRA). Received September 13, 2021.

PCA9685 PWM Driver Board. Replacing the functionality usually provided by the PixHawk which was now used just for sensor interface and sensor fusion. The normalized control inputs are mapped to the PWM signals.

The zero thrust occurs with the PWM signal of 1500 (b_0) yet there exits a dead-zone region where no thrust is received [21]. Thus, an inverse dead-zone, as in [22], was implemented to the mapped PWM signals as

$$pwm = D_{inv}(u_i) = \begin{cases} \frac{u_i - b_0}{\sigma_r} u_i + b_r & u_i > b_0, \\ b_0 & u_i = b_0, \\ \frac{u_i - b_0}{\sigma_l} u_i + b_l & u_i < b_0, \end{cases}$$

where σ_i and b_i denote the dead-zone slope characteristics and breakpoints for the left and the right ($i = l, r$) thresholds, respectively.

TABLE I

CONTROLLER PARAMETERS UTILIZED DURING THE EXPERIMENTS

PID	$k_p^x = k_p^y = 60$ $k_p^z = 120$	$k_i^j = 2$ $(j = x, y, z)$	$k_d^x = k_d^y = 200$ $k_d^z = 410$
	$k_p^\psi = 5$	$k_i^\psi = 0.5$	$k_d^\psi = 25$
SMC	$k_p^x = k_p^y = 50$ $k_p^z = 110$	$k_i^x = k_i^y = 5$ $k_i^z = 2$	$k_d^x = k_d^y = 150$ $k_d^z = 350$
	$k_p^\psi = 0.1$	$k_i^\psi = 0.1$	$k_d^\psi = 0.5$
	$\bar{m}_x = \bar{m}_y = 1.5$ $\bar{m}_z = 3$ $\bar{m}_\psi = 0.1$	$\mu = 0.01$ $\beta = 10^{\ 5}$ $k_s = 0.2$	$\delta = 0.001$ $\delta_d = 200$ $\delta_c = 100$

III. RESULTS

The designed controllers, (2) and (3), were evaluated in two experiments by using the controller parameters given in Table I, with different trajectories and environmental disturbances (i.e., waves) in respective experiment. Detailed information about how to tune such SMC controller is proposed in [19], yet here additional k_s positive parameter ($k_s \leq 1$) was included to penalize the effect of a large time delay estimation error due to the slow measurement rate. The scaling factor was incrementally increased until further increase would deteriorate the overall performance. And the PID gains were tuned heuristically.

In the first experiment, the vehicle followed a circular trajectory as $x_r = x_0 + a_r cos(\omega t) - a_r$ and $y_r = y_0 + a_r sin(\omega t)$ with a $1\,\mathrm{m}$ radius and $\omega = 0.1\,\mathrm{rad\,s^{-1}}$ in a fixed heave position relative to the tank floor (approximately $0.5\,\mathrm{m}$ below the water surface), similar to the case in [14]. A sinusoidal type wave with an amplitude approximately equal to $0.4\,\mathrm{m}$ was used as a disturbance.

In surveillance operations, the position and attitude control of the vehicle is crucial as the quality of the inspection data is highly dependent on the motion of the vehicle. In the second experiment, it was assumed that the vehicle needed to inspect a submerged structure via a vertical motion with a fixed surge, sway, and yaw. The vehicle continuously followed an up-down trajectory in heave, $z_r = z_0 + a_z sin(\omega_z t)$, with an amplitude equivalent to $0.5\,\mathrm{m}$ and angular frequency equal to $0.2\,\mathrm{rad\,s^{-1}}$ in the centre of the pool. To simulate the distorted motion of the waves around a submerged structure, a centralized type wave, where maximum wave occurred in the centre of the pool, was used as an environmental disturbance with an amplitude approximately $0.45\,\mathrm{m}$. In both experiments, it was assumed that there existed a time delay within the communication channel such that the round trip time delay was equal to $200\,\mathrm{ms}$ by implementing virtual buffers into the feedback loop.

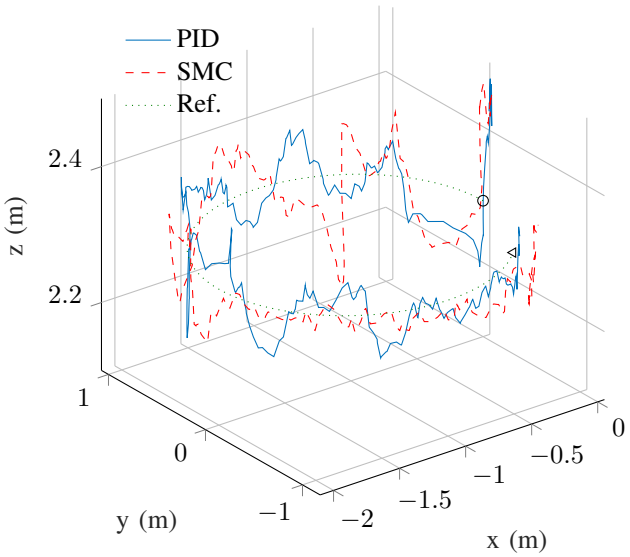

Fig. 5. Underwater ROV position in the inertial reference frame (with normalized x and y) during the circular motion under the sinusoidal disturbances with different controllers. Vehicle faced always towards the motion direction via yaw controller.

The circular motion of the vehicle while under the influence of the sinusoidal waves and with the communication time delay is illustrated in Fig.5, where the initial positions in surge and heave are normalized for comparison. The heave illustrates the relative distance of the ROV to the pool floor and the vehicle is faced towards the motion direction with the help of the yaw controller. Despite the disturbances and time delay within the communication channel, both controllers could execute a satisfactorily comparable trajectory.

TABLE II

EUCLIDEAN NORM OF THE POSITION ERROR FOR x, y, z, AND ψ

	Circular Motion		Vertical Motion	
	PID	SMC	PID	SMC
$\|E_{xyz\psi}\|$	6.8349	3.9051	7.8494	5.2695

For the circular motion, the position error and control efforts in the controlled directions are illustrated in Fig. 6 and Fig. 7, respectively. The SMC illustrates better performance as $\|E_{xyz\psi}\|$ is approximately 33% less than that with the PID controller, as shown in Table II.

With both controllers, the maximum position error remains less than $0.2\,\mathrm{m}$ in the surge and sway. Better performance was obtained in heave and yaw where the steady-state error is less than $0.05\,\mathrm{m}$ and $0.05\,\mathrm{rad}$, respectively, as seen Fig. 6.

Inspecting submerged structures, such as offshore windmill bases, is difficult due to the turbulent flow around the structure. The designed controller needs to have a robust performance under such extreme disturbances to avoid any

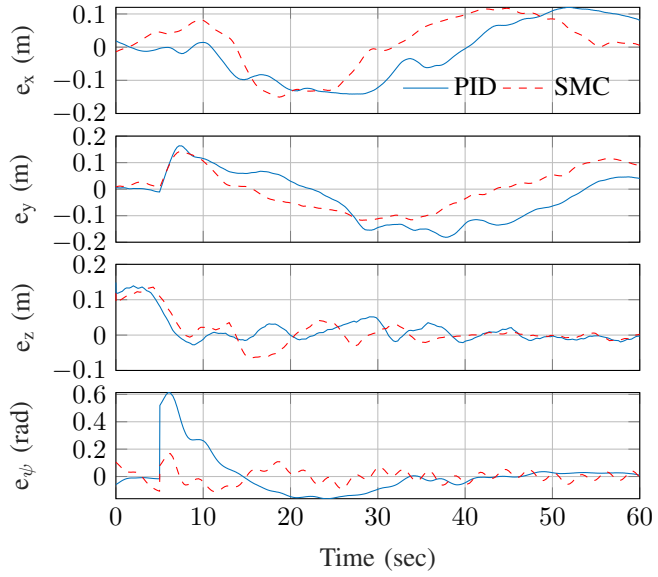

Fig. 6. The ROV's position and orientation errors in the inertial reference frame during the circular motion under the sinusoidal disturbances.

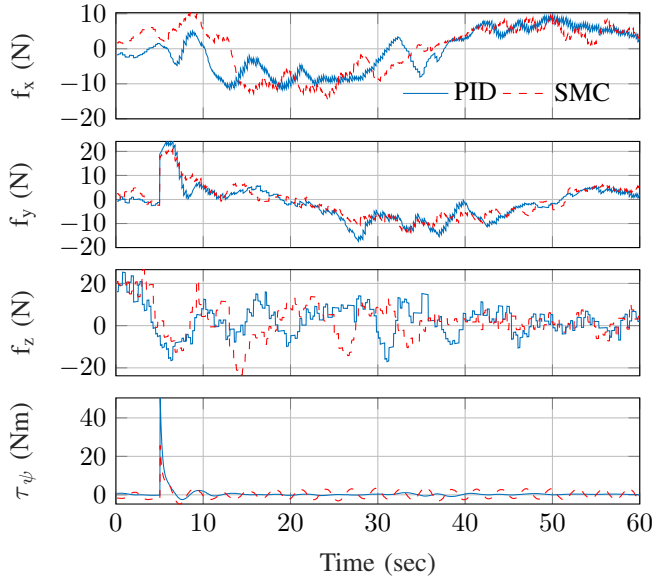

Fig. 7. Control efforts in the inertial frame during the circular motion under the sinusoidal disturbances.

undesired collusion. In the second experiment, the central wave was implemented to mimic such conditions where the intensity of the waves were increased over time and the maximum disturbance occurred after 20 s within the experiment.

In the second experiment, the SMC shows significantly better performance than the PID controller as the $\|E_{xyz\psi}\|$ is 42% better than with the latter one (Table II). With the PID controller the performance deteriorates significantly as disturbances increase, as seen in Fig. 8 where the steady state error surges in PID controller after 20 s in parallel to the wave magnitude. With the SMC, on the other hand, the steady state error remains low despite the increase in the disturbance.

Additionally, the better performance with the SMC is

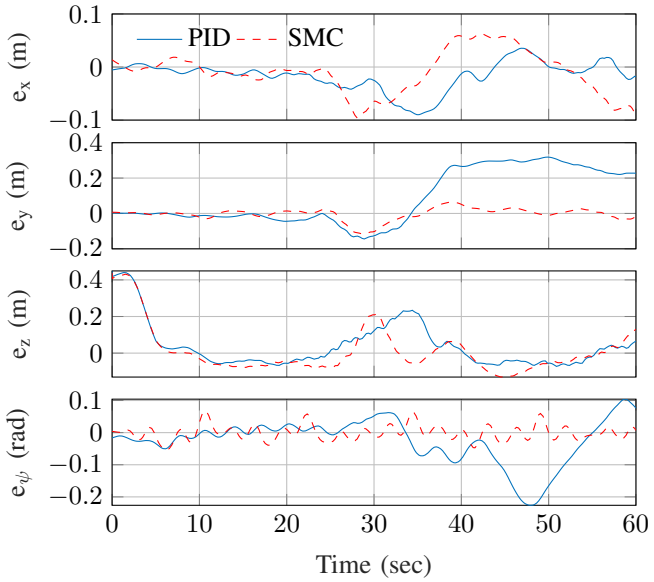

Fig. 8. The ROV's position and orientation errors in the inertial frame during the vertical surface inspection test under the extreme disturbances.

obtained even with less control effort as seen in Fig. 9. Reducing the control effort in a UUV without any detrimental effect on the performance is important for two reasons. Firstly, the underwater vehicles are mainly battery-powered; thus, to increase the operational duration the controller should be energy efficient. Secondly, only limited amount of power/torque can be generated by the thrusters and the vehicle should use this narrow power range effectively to deal with the disturbances.

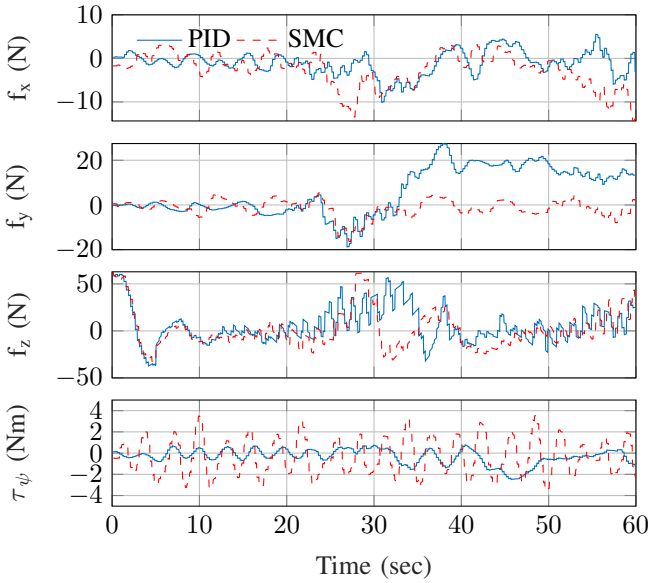

Fig. 9. Control efforts in the inertial frame during the vertical surface inspection under the extreme disturbances.

IV. Conclusion

This paper experimentally illustrates the feasibility and effectiveness of a SMC based time-delay control as a robust controller for an underwater vehicle. A SMC with a delay

estimation term was implemented to control the position and heading of an underwater vehicle under external disturbances and in the presence of communication time delays. The proposed controller was compared to a standard PID controller conventionally used in underwater vehicle control. With the proposed SMC with delay estimation term, the disturbances were better attenuated with less control effort. The power of the proposed controller was most pronounced with the vertical surface inspection experiment under extreme disturbance, as deviation from the desired position/heading and control effort were significantly less with the proposed controller in comparison to the standard PID controller. Correspondingly, the proposed controller can attenuate and suppress fast-varying disturbances with minimal steady-state error and control efforts; thus, showing better control precision than the PID controller under external disturbances. The results are promising that underwater structures can be inspected with an ROV utilizing such controller despite disturbances affecting the system.

REFERENCES

[1] E. Bovio, D. Cecchi, and F. Baralli, "Autonomous underwater vehicles for scientific and naval operations," *Annual Reviews in Control*, vol. 30, no. 2, pp. 117–130, 2006.

[2] T. I. Fossen, K. Y. Pettersen, and R. Galeazzi, "Line-of-sight path following for dubins paths with adaptive sideslip compensation of drift forces," *IEEE Transactions on Control Systems Technology*, vol. 23, no. 2, pp. 820–827, 2015.

[3] J. Kim, H. Joe, S. C. Yu, J. S. Lee, and M. Kim, "Time-delay controller design for position control of autonomous underwater vehicle under disturbances," *IEEE Transactions on Industrial Electronics*, vol. 63, no. 2, pp. 1052–1061, 2016.

[4] R. Prasanth Kumar, A. Dasgupta, and C. S. Kumar, "Robust trajectory control of underwater vehicles using time delay control law," *Ocean Engineering*, vol. 34, no. 5-6, pp. 842–849, 2007.

[5] B. Jalving, "The NDRE-AUV flight control system," *IEEE Journal of Oceanic Engineering*, vol. 19, no. 4, pp. 497–501, 1994.

[6] P. Herman, "Decoupled PD set-point controller for underwater vehicles," *Ocean Engineering*, vol. 36, no. 6, pp. 529–534, 2009.

[7] T. I. Fossen and S. I. Sagatun, "Adaptive control of nonlinear underwater robotic systems," *Modelling, Identification and Control*, vol. 12, no. 2, pp. 95–105, 1991.

[8] M. L. Corradini and G. Orlando, "A discrete adaptive variable-structure controller for MIMO systems, and its application to an underwater ROV," *IEEE Transactions of Control System Technology*, vol. 5, no. 3, pp. 349–359, 1996.

[9] G. Antonelli, F. Caccavale, S. Chiaverini, and G. Fusco, "A novel adaptive control law for underwater vehicles," *IEEE Transactions on Control Systems Technology*, vol. 11, no. 2, pp. 221–232, 2003.

[10] S. Mohan and J. Kim, "Indirect adaptive control of an autonomous underwater vehicle-manipulator system for underwater manipulation tasks," *Ocean Engineering*, vol. 54, pp. 233–243, 2012.

[11] K. Cetin, C. S. Zapico, H. Tugal, Y. Petillot, M. Dunnigan, and M. S. Erden, "Application of Adaptive and Switching Control for Contact Maintenance of a Robotic Vehicle-Manipulator System for Underwater Asset Inspection," *Frontiers in Robotics and AI*, vol. 8, pp. 1–22, 2021.

[12] J. Biggs and W. Holderbaum, "Optimal kinematic control of an autonomous underwater vehicle," *IEEE Transactions on Automatic Control*, vol. 54, no. 7, pp. 1623–1626, 2009.

[13] L. Qiao, S. Ruan, G. Zhang, and W. Zhang, "Robust H2 optimal depth control of an autonomous underwater vehicle with output disturbances and time delay," *Ocean Engineering*, vol. 165, pp. 399–409, 2018.

[14] J. Xu, M. Wang, and L. Qiao, "Dynamical sliding mode control for the trajectory tracking of underactuated unmanned underwater vehicles," *Ocean Engineering*, vol. 105, pp. 54–63, 2015.

[15] K. Tanakitkorn, P. A. Wilson, S. R. Turnock, and A. B. Phillips, "Sliding mode heading control of an overactuated, hover-capable autonomous underwater vehicle with experimental verification," *Journal of Field Robotics*, vol. 35, no. 3, pp. 396–415, 2018.

[16] H. Zhou, K. Liu, Y. Li, and S. Ren, "Dynamic sliding mode control based on multi-model switching laws for the depth control of an autonomous underwater vehicle," *International Journal of Advanced Robotic Systems*, vol. 12, 2015.

[17] M. L. Corradini, A. Monteriu, and G. Orlando, "An actuator failure tolerant robust control approach for an underwater remotely operated vehicle," *IEEE Transactions of Control System Technology*, vol. 19, no. 5, pp. 1036–1046, 2011.

[18] T. I. Fossen, *Handbook of marine craft hydrodynamics and motion control*. John Wiley & Sons, 2011.

[19] X. Han, I. Kucukdemiral, and M. S. Erden, "Time delay control with sliding mode observer for a class of non-linear systems: performance and stability," *International Journal of Robust and Nonlinear Control, in press*, 2021.

[20] F. Piltan, B. Boroomand, A. Jhaed, and H. Rezaie, "Methodology of mathematical error-based tuning sliding mode controller," *International Journal of Control and Automation*, vol. 6, no. 2, pp. 96–117, 2012.

[21] "BlueRobotics." [Online]. Available: https://bluerobotics.com/store/thrusters/t100-t200-thrusters/t200-thruster-r2-rp/

[22] J. D. J. Rubio, Z. Zamudio, J. Pacheco, and D. Mújica Vargas, "Proportional derivative control with inverse dead-zone for pendulum systems," *Mathematical Problems in Engineering*, vol. 2013, 2013.